






Article

Human-Altered Soils at an Archeological Site of the Bronze Age: The Tyater-Araslanovo-II Settlement, Southern Cis-Ural Region, Russia

Ruslan Suleymanov ¹, Gulnara Obydenova ², Andrey Kungurtsev ^{3,4}, Niyaz Atnabaev ², Mikhail Komissarov ¹, Artyom Gusarov ^{5,*}, Ilgiza Adelmurzhina ⁶, Azamat Suleymanov ⁷ and Evgeny Abakumov ⁸

- ¹ Laboratory of Soil Science, Ufa Institute of Biology UFRS, Russian Academy of Sciences, Pr. Oktyabrya 69, 450054 Ufa, Russia; soils@mail.ru (R.S.); mkomissarov@list.ru (M.K.)
 - ² Department of General History and Cultural Heritage, Bashkir State Pedagogical University Named after Akmulla M., October Revolution 3-a, 450008 Ufa, Russia; Gto1104@mail.ru (G.O.); niaz-02@bk.ru (N.A.)
 - ³ Department of Earth and Space Sciences, Ural Federal University Named after the First President of Russia B.N. Yeltsin, Mira 19, 620002 Yekaterinburg, Russia; jajk@yandex.ru
 - ⁴ Department of Ecology and Life Safety, Bashkir State University, Zaki Validi 32, 450076 Ufa, Russia
 - ⁵ Institute of Geology and Petroleum Technologies, Kazan Federal University, Kremlyovskaya Str. 18, 420008 Kazan, Russia
 - ⁶ Department of Geodesy, Cartography and Geographic Information Systems, Bashkir State University, Zaki Validi 32, 450076 Ufa, Russia; adelmur@mail.ru
 - ⁷ Department of Environmental Protection and Prudent Exploitation of Natural Resources, Ufa State Petroleum Technological University, Kosmonavtov St. 1, 450064 Ufa, Russia; filpip@yandex.ru
 - ⁸ Department of Applied Ecology, Saint Petersburg State University, 16 Line 29 Vasilyevskiy Island, 199034 Saint Petersburg, Russia; e_abakumov@mail.ru
- * Correspondence: avgusarov@mail.ru



check for updates

Citation: Suleymanov, R.; Obydenova, G.; Kungurtsev, A.; Atnabaev, N.; Komissarov, M.; Gusarov, A.; Adelmurzhina, I.; Suleymanov, A.; Abakumov, E.

Human-Altered Soils at an Archeological Site of the Bronze Age: The Tyater-Araslanovo-II Settlement, Southern Cis-Ural Region, Russia. *Quaternary* **2021**, *4*, 32. <https://doi.org/10.3390/quat4040032>

Academic Editors: David Psomiadis and Antonios Mouratidis

Received: 21 July 2021

Accepted: 12 October 2021

Published: 15 October 2021

Publisher's Note: MDPI stays neutral with regard to jurisdictional claims in published maps and institutional affiliations.



Copyright: © 2021 by the authors. Licensee MDPI, Basel, Switzerland. This article is an open access article distributed under the terms and conditions of the Creative Commons Attribution (CC BY) license (<https://creativecommons.org/licenses/by/4.0/>).

Abstract: This paper presents the results of studying the soils at the archeological site of the Tyater-Araslanovo-II settlement located in the Republic of Bashkortostan, eastern European Russia. The settlement functioned in the 15th–12th centuries BCE (the Late Bronze Age). We compared the soil properties at four sites in the study area: archeological (1), buried (2), affected by long pyrogenic exposure (3), and background site (4). In soil samples, the total carbon content, the fractional composition of humus and organic matter characteristics, alkaline hydrolyzable nitrogen, total phosphorus, mobile phosphorus, potassium, absorbed calcium and magnesium, pH, particle size distribution, basal soil respiration, and optical density were estimated. The study results showed the anthropogenic impact on the archeological site's soils. The newly formed AU horizon at the archeological site (1), affected by the cattle summer camp, was richer in soil nutrients and agrochemical properties, namely, the content of exchangeable and gross forms of phosphorus, alkaline hydrolyzable nitrogen, and exchange cations of the soil absorbing complex compared to the reference soil (4). For the pyrogenic layer (AU[hh]_{pyr}) from the ancient furnace (fireplace) (3), the mobile and total forms of phosphorus were several times higher than those in the reference soil (4) but inferior regarding other agrochemical parameters. Thus, the activities of ancient people (especially cattle breeding) greatly influenced the properties of the soil.

Keywords: ancient settlement; soil properties; organic substances; basal respiration; optical density

1. Introduction

Throughout history, human development has significantly impacted the environment and soil cover. In the relationship between humans and the pedosphere, the importance of soil is to meet the ever-increasing demand for food and water, energy, and natural resources [1]. Therefore, ancient people tried to settle in areas with fertile soil [2] or used organic waste as fertilizer in conditions of limited fertility [3]. As early as 2000 years ago in

China, people studied soils' classification, distribution, and agricultural use [4]. The vital activity of ancient humans was accompanied by the transformation of the soil cover. In the soil layers of ancient settlements, ancient soils have been preserved by which one can judge the natural and anthropogenic conditions of the time when they were formed [5,6]. This evidence is contained in the form of various new mineral formations, soil humus, and fragments of plant and animal organisms [7–10].

Recently, it has become possible to interpret the “features of life” of ancient people, including the settlement structure, land-use methods, and evidence of anthropogenic impact on the soil and landscape [11–13]. Archeological soil science allows for solving this problem. Modern archeological research is the integration of geosciences into archeology in addition to current research methods that are accepted in genetic soil science [14]. This research examines the current state of soils and evaluates the changes in the basic properties of soils under the influence of the vital activity of ancient people at an archeological site of one of the cultural and historical log-house settlements of the Bronze Age in the Cis-Ural region of Europe.

2. Study Area

The archeological site of the Tyater-Araslanovo-II Settlement is located in the Sterlibashevsky district of the Republic of Bashkortostan, Russia (Figure 1), 360 m north of the village with the same name, on the low right bank of the Tyater River (Figure 2). The settlement was discovered in 1970 by A. Pshenichnyuk, and archeological excavations started in 2017. An archeological plot (Figure 3) was deployed, and the excavation area amounted to about 120 m². A total of 2047 units of finds were obtained during the settlement study: 580 fragments of ceramics, 493 units of stones and pebbles, 14 pieces of burnt clay, 10 individual finds, 10 units including shells, pieces of ocher, and 940 units of archeological material.



Figure 1. Location of the Tyater-Araslanovo-II Settlement archeological site.

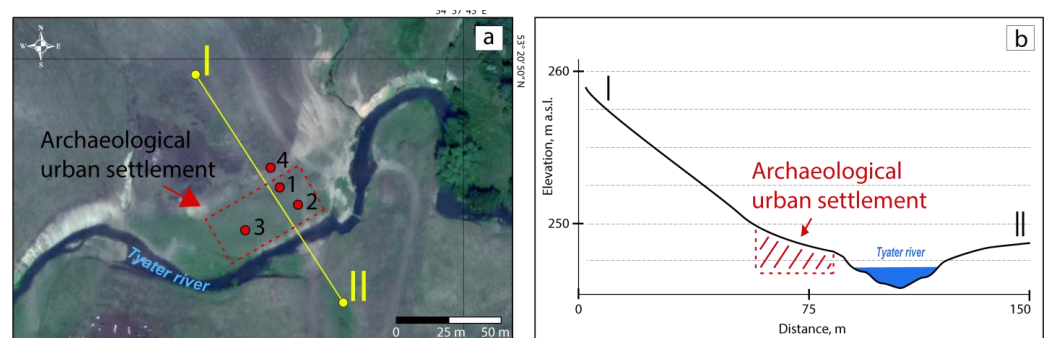


Figure 2. (a) Soil pit sites 1–4 (see also Figure 3) and (b) longitudinal profiles I–II at the Tyater-Araslanovo-II settlement archeological site.

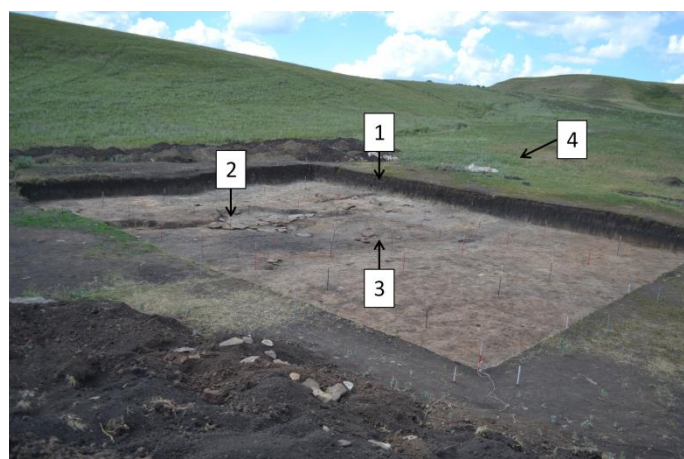


Figure 3. General view of the Tyater-Araslanovo-II settlement archeological site and location of the studied soil pits.

The ceramic collection of the settlement is represented by fragments of the brown and dark gray pots. Chamotte, small shells, and plant impurities were used as leaners. Individual finds are represented by two whetstones, a spindle made of the ceramic wall, bone spindles, and kochedyk (pile) from animal ribs, a blank for the arrowhead. We used special reference books and atlases to determine the age and species composition [15–17]. As a comparative material, we used published studies on osteological collections of the Late Bronze Age of the Volga-Ural region, which approximately demonstrated the same species and age composition of the herd of the ancient population [18,19]. The archeozoological collection is represented by eight species, with five of them being domestic animals, namely, cow (*Bos taurus Taurus* (Linnaeus, 1758)), sheep (*Ovis aries* (Linnaeus, 1758)), goat (*Capra hircus* (Linnaeus, 1758)), horse (*Equus* (Linnaeus, 1880)), and pig (*Sus scrofa Domestica* (Linnaeus, 1758)), and three being wild animals, namely, steppe marmot (*Marmota Bobak* (Müller, 1776)), squirrel (*Spermophilus* (Cuvier, 1825)), and fox (*Vulpes* (Linnaeus, 1758)).

The findings and remains of the animals suggest that the site belongs to one of the cultural and historical log-house communities, and the time of its existence dates roughly back to the 15th–12th centuries BCE (the Late Bronze Age). According to Golyeva et al. [20], the Tyater-Araslanovo-II settlement was built by the ancient people of the Srubno-Alakul archeological culture of the Late Bronze Age (1890–1750 cal BCE). Another ancient settlement of the Late Bronze Age in the Urals, Muradymovo, located near Tyater-Araslanovo-II (~70 km southeast), also belonged to the Srubno-Alakul archeological culture (1750–1350 years BCE cal) and had a tradition of building their houses from gypsum rocks [21]. Krzewinska et al. [22] reported that the Late Bronze Age on the territory of Southern Trans-Urals (1890–1750 BC) is generally characterized by two major archeological cultures and population groups: Srubnaya and Andronovskaya (Alakul culture and Fyodorovskaya). The contact of these two distinct cultural groups constituted a special mix of material culture, carrying both typical features of the Srubnaya and Andronovskaya cultures and developing local features. Krzewinska et al. [22] and Shuteleva et al. [23] used radiocarbon with a combination of paleoclimatic investigations for chronological detection and date calibration. Such a method provided information on the more specific chronological borders of archeological monuments (c. 1890–1750 BCE). These data were collected in recent investigations of settlements and mounds of the Late Bronze Age in southern Trans-Urals. The obtained results refined the chronological framework and pushed the boundaries by c. 150–200 years.

Environmental Characteristics of the Study Area

The territory of the research area is located in the southern forest–steppe subzone. The climate is characterized by a continental climate with moderate humidity (Dfb according to the climate classification of Köppen–Geiger [24]). Annual precipitation is in the range

of 360–490 mm. Average annual air temperature is in the range of 1.7–2.6 °C; average air temperature in January is –14 to –15.5 °C and 18–20 °C in July. The relief is a plateau-like upland, bounded by steep slopes in some places, which is crossed by small rivers deeply cut into Permian rocks (clays, sandstones, marls, limestones, and dolomites). The valleys of many rivers have a canyon-like shape with steep slopes. The heterogeneity of the relief and human activity influenced the formation of vegetation. Forest vegetation is represented by birch, oak, birch–aspen, and oak–birch forests, and pine forests have been preserved on elevated relief elements. The steppe territories are plowed up to 45–60% of their original area. Natural vegetation is represented by meadows and mixed steppe grasses, mainly feather grass. Soil cover in the study region is represented by Haplic Chernozems, Luvic Chernozems, and Haplic Phaeozems according to the WRB [25]. On steep slopes, there are eroded soils with a small thickness of the humus horizon. In the floodplains of the region's rivers, there are Gleyic Fluvisols, Skeletic Fluvisols, and Salic Vertisols [25,26].

3. Materials and Methods

Three soil pits were laid inside the archeological plot, and one pit was excavated nearby outside (see Figure 3). From each pit, samples were taken mainly from the genetic horizons (see Table 1 and Figure 4). Soil samples were dried in an oven at 90 °C to constant weight, crushed in a mortar, and sieved by 2 mm mesh. Then, the following analyses and measurements were carried out. Organic carbon content was determined by Tyurin (wet combustion) [27]; fractional composition of humus and characteristics of organic matter by Orlov [28], humus type by Kononova [29]; alkaline hydrolyzable nitrogen by Kornfield [27]; total phosphorus by Ginzburg [27]; mobile phosphorus and potassium by Chirikov (0.5 mol L⁻¹ CH₃COOH was extracted at a 1.0:2.5 soil/solution ratio) [27]; absorbed calcium and magnesium by the trilonometric method; soil reaction by potentiometry (in 1 mol L⁻¹ KCl suspension (1.0:2.5 soil/solution)) [27]; particle size distribution by the Kachinsky standard sedimentation method [30]. Soil basal respiration was determined by the rate of CO₂ release from the soil samples during its 48-h incubation at 22 °C [31]. Geomorphometric analysis of the study site was carried out using the QGIS geographic information system based on a digital elevation model (<https://www2.jpl.nasa.gov/srtm>, accessed on 12 October 2020).

4. Results and Discussion

4.1. Soil-Pit Characteristics and Morphological Description

The territory of the archeological site is located in the valley of the Tyater River within a flat ledge (the bottom of a steep slope) measuring 90 × 30 m with a slight gradient towards the river (see Figure 3). Capillary rise in groundwater in rivers, water runoff from overlying relief elements, and periodic moistening by melt and rainwater determine the water regime of the soil as the dominant factor in the genesis of the soil cover. In this connection, the soil within the aligned ledge was diagnosed as Gleyic Fluvisols [25].

Below is a morphological description of the pits laid in the territory of the archeological site.

Soil Pit 1 (Figure 4a). Place: The right side of the Tyater River valley, the bottom of a steep slope, the north wall of archeological plot excavation. Location: 53.347927 N, 54.960789 E. The following soil horizons were identified:

- AU, 0–12 cm. Dark gray, fine-grained, crumbly, moist, sandy clay loam (morphological description of soil texture was determined by feel); smooth transition in color.
- AUrr*, 12–21 cm. Light brown, dusty, crumbly, dry, sandy clay loam, inclusions of organic residues with a high degree of decomposition and fine gravel; transition to the next horizon is wavy in color.
- AU[hh], 21–69 cm. Dark gray, coarse-grained, loose, dry, sandy loam with inclusions of fragments of animal bones and fine gravel; transition to the next horizon is even in color.
- Q, 69–83 cm. Light bluish, large–medium prismatic, friable, dry, medium loamy with Fe–Mn nodules; carbonate impregnation; effervescence with 10% HCl.

- CQ, 83–100 cm. Bluish-brown, structureless, moist, silt loam with Fe–Mn nodules; carbonate impregnation; effervescence with 10% HCl.

* The formation of the AUrr horizon was because, in the 1950s–1960s, a summer cattle camp existed in the archeological site area. The waste of their livelihoods was not taken out and accumulated on the spot. Subsequently, the waste was covered by deposits formed due to water erosion caused by intensive grazing in areas located higher up the slope.

Soil Pit 2 (fragment) (Figure 4b). By the time the soil was studied, the modern humus accumulation horizon had been removed due to archeological excavations. In the center of the excavations, sandstone boulders were found, under which fragments of the buried soil horizon of humus accumulation were preserved. This horizon probably existed during the functioning of the settlement. Below is a morphological description of the pit.

- AU[hh], 42–70 cm. Dark gray, moist, powdery, crumbly, silt loam.
- Q, 70–85 cm. Bluish-red, dense, wet, with inclusions of reddish sand grains and fine gravel, structureless, sticky; effervescence with 10% HCl.

Soil Pit 3 (fragment) (Figure 4c). In addition, during archeological excavations, a place with clear signs of prolonged exposure to high temperatures (a fireplace used for cooking or heating a house) was found from where soil samples were taken for chemical analysis. Below is a morphological description of the pit's horizons.

- AU[hh]_{pyr}, 63–74 cm. Heterogeneously colored reddish-bluish-brown, structureless, silty and sticky clay loam.

Soil Pit 4 (Figure 4d). Reference soil (Gleyic Fluvisols), 10 m north of pit 1.

- AU, 0–70 cm. Dark gray, medium–coarse-grained, friable, moist, sandy clay loam with a smooth transition in color to the lower horizon.
- Q, 70–90 cm. Light bluish, coarse–medium prismatic, friable and dry silt loam with dark gray streaks in the form of tongues from the overlying horizon; Fe–Mn nodules and carbonate impregnation; effervescence with 10% HCl.
- CQ, 90–120 cm. Bluish-brown, structureless and moist loam with Fe–Mn nodules and carbonate impregnation; effervescence with 10% HCl.

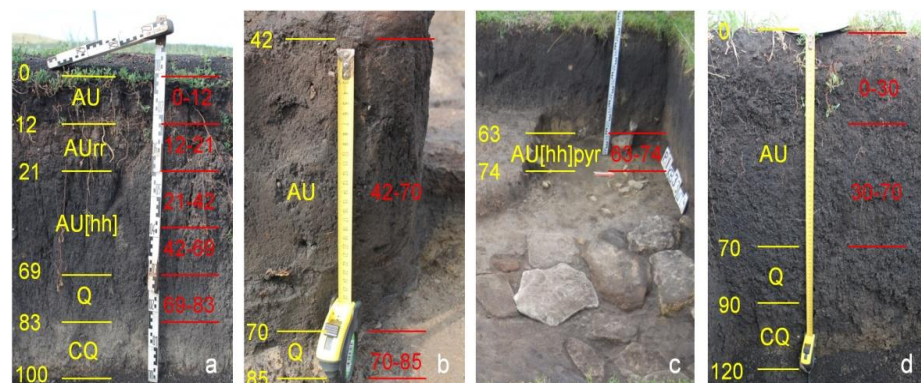


Figure 4. Soil profile views: (a) Soil Pit 1; (b) Soil Pit 2; (c) Soil Pit 3; (d) Soil Pit 4. Genetic horizons are in yellow; Sampling depths (cm) are in red.

4.2. Particle Size Distribution

Soil texture (particle size distribution) is one of the fundamental physical factors that affect various soil properties [32,33]. Analysis of particle size distribution (Figure 5) showed that the fine fractions prevail in the upper layers of the reference soil (Soil Pit 4). For example, in the AU humus horizon (0–30 cm), their values were about 65% (silt ~57%, clay ~8%); the lowest proportion is represented by the sand fraction, ~35%. With depth, clay content increases to ~34% due to decreased sand content (~7%), while the proportion of silt remains practically unchanged. According to the USDA classification, the soil composition in the humus horizon of the reference soil varies with depth from silt

loam to silty clay loam. A similar distribution of fractions in the profiles of Fluvisols was noted [34]. The granulometric composition of soils is not affected by their position in the relief (slope or plateau).

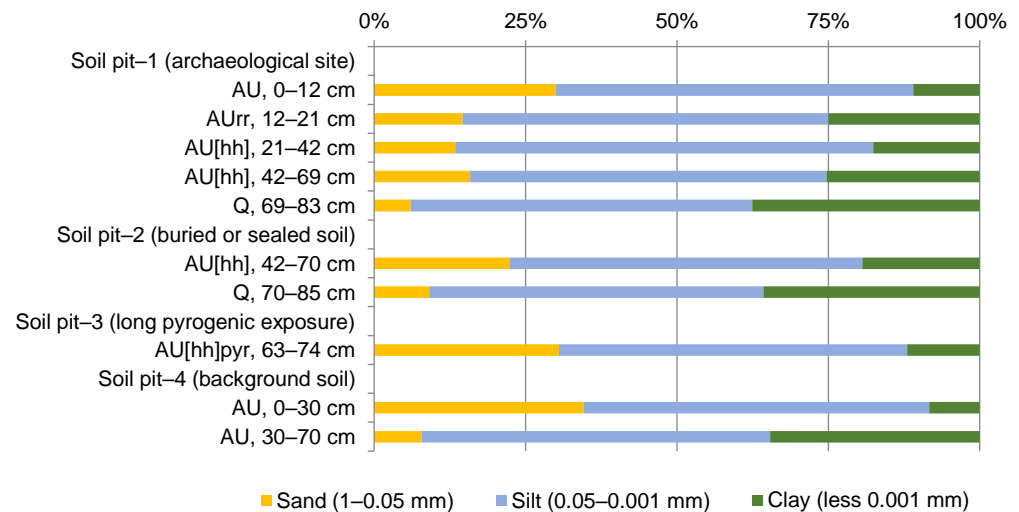


Figure 5. Particle size distribution in the studied pits' soils.

In the upper horizon of the soil profile at the archeological site (Soil Pit 1), the proportion of the sand fraction (~30%) exceeds the clay fraction (~11%), but silt (~59%) predominates. With increasing depth, there is also a gradual decrease in the sand content and an increase in the proportion of clay fraction with a relatively stable clay fraction content. The soil texture varies from silt loam in the upper horizon to silty clay loam in the quasigley horizon Q, 69–83 cm. The same change in the ratio of fractions was noted in the buried soil (Soil Pit 2), where the granulometric composition varies with depth from silt loam to silty clay loam; In the pyrogenic layer, the soil texture was characterized as silt loam.

4.3. Chemical Properties

The humus accumulation horizon (AU) of the reference Gleyic Fluvisols (Soil Pit 4) is characterized by a neutral pH reaction in both layers of depths of 0–30 and 30–70 cm. The content of organic matter decreases with depth (Table 1). A similar distribution trend was also found for alkaline hydrolyzable nitrogen, total phosphorus, and mobile forms of phosphorus and potassium. Exchangeable cations do not change along with the depth of the soil profile, but the proportion of calcium in their composition is higher.

In the soil profile of Pit 1, some acidification in the upper horizons AU (0–12 cm) and AUrr (12–21 cm) was observed. Compared to the background plot, pH was lower by 0.3–0.5 units. This was obviously due to the influence of organic waste (manure) forming due to grazing. This is also the reason for the predominant organic carbon and nutrient content. The buried humus horizon AU[hh] (21–69 cm) is characterized by a neutral pH reaction. In this layer, the predominant content of nutrients is also associated with the vital activity of ancient humans. Holliday et al. [35] and Rodrigues et al. [36] believe that phosphorus in the soil is an essential indicator of the activity of ancient people and livestock.

In general, soils of archeological sites are characterized by an excess of biogenic elements compared to reference soils. For example, in the southwest of Greenland, the contents of P, NO₃, and NH₄ in archeological deposits were 2–6 times higher than those in the surrounding soils [37]. In some cases, increased content of biogenic and organic substances results in the formation of archeological chernozems, which may even serve as the basis for a subsistence economy [38–40]. In our study, organic carbon content was 0.7% less on average than in the modern reference soil, which is probably associated with diagenetic processes [41,42].

Table 1. Chemical properties and basal respiration (BR, $\mu\text{g CO}_2\text{-C g}^{-1}\text{soil h}^{-1}$) of the archeological site's soil.

Horizon and Sampling Depth, cm	C_{org} , %	BR	Ca^{2+}	Mg^{2+}	$\text{Ca}^{2+} + \text{Mg}^{2+}$	P_2O_5		N, Alkaline Hydrolyzable	K_2O , Mobile	pH (H_2O)
			$\text{cmol}_{(+)}\text{ kg}^{-1}$			Total	Mobile			
Soil Pit 1 (archeological site)										
AU, 0–12	8.79	1.31	46	9	55	3176	86.9	588	320	6.9
AUrr, 12–21	8.33	2.98	38	6	44	2643	95.3	756	550	6.7
AU[hh], 21–42	6.17	1.04	38	14	52	2746	93.1	280	275	7.4
AU[hh], 42–69	3.77	0.78	37	14	51	2316	99.4	182	220	7.0
Q, 69–83	1.46	0.22	36	6	42	1332	69.0	70	85	7.0
Soil Pit 2 (buried or sealed soil)										
AU[hh], 42–70	2.33	0.34	34	7	41	7602	96.2	140	800	7.4
Q, 70–85	0.54	0.23	35	9	44	1619	101.2	42	115	7.3
Soil Pit 3 (long pyrogenic exposure)										
AU[hh] _{pyr} , 63–74	1.06	0.21	27	7	34	8135	92.2	98	1400	7.4
Soil Pit 4 (reference soil)										
AU, 0–30	7.82	1.29	40	9	49	2131	76.9	420	210	7.2
AU, 30–70	3.41	0.97	40	8	48	1045	34.4	168	75	7.2

Fire is an influential environmental factor affecting all soil properties [43,44]. In some cases, fire can increase nutrients [45], electrical conductivity, total phosphorus, and mobile potassium. All this finally results in a reduction in total nitrogen and organic matter [46]. With decreasing soil organic matter, other changes also occur in chemical properties, including humic (HA) and fulvic acids (FA). New compounds are also formed with high resistance to oxidation and biological degradation [47,48].

The long-term pyrogenic effect significantly influenced the properties of the quasigley horizon AU[hh]_{pyr}, 63–74 cm (Soil Pit 3). First, there was a significant increase in the content of mobile potassium (up to 1400 mg kg^{-1}) and total phosphorus (up to 8135 mg kg^{-1}) in the soil compared to the soil profile of the archeological site, where these components differ in the ranges of 85–550 and $1332\text{--}3176\text{ mg kg}^{-1}$ respectively. There was also a decrease in the number of exchangeable cations, mainly due to changes in Ca^{2+} , up to $34\text{ cmol}_{(+)}\text{ kg}^{-1}$ of soil. The rest of the studied soil parameters did not significantly change. Such a high content of soil nutrients in the hearth was probably due to the accumulation of ash, unburned wood, and other organic materials (remains of food, vegetation, and animal bones) in this place. Earthworms and rodents could also dwell there, followed by the formation of feces or their remains.

The buried and sealed soil under the sandstone boulders (Soil Pit 2) is also characterized by an increased content of mobile potassium (800 mg kg^{-1} of soil) and phosphorus (7602 mg kg^{-1} of the soil) in its humus horizon. It also indicates the impact of ancient humans' vital activity in this area. Soil organic carbon content due to diagenesis decreased to 2.33%.

Basal respiration is one of the indicators of microbial communities' activity. It reflects the intensity of mineralization of organic matter in the soil [49,50]. The maximum rate of basal respiration ($2.98\text{ }\mu\text{g CO}_2\text{-C g}^{-1}\text{ soil h}^{-1}$) was observed in the archeological site (Soil Pit 1) at the AUrr horizon (12–21 cm). The formation of this horizon was influenced by the functioning of the cattle summer field camp, which is associated with a large number of organic residues. In the upper part of the soil profile (0–12 cm), in the AU horizon of humus accumulation, basal respiration rates correspond with reference soil rates (Soil Pit 4, AU, 0–30 cm). With depth, there was a decrease to $0.78\text{ }\mu\text{g CO}_2\text{-C g}^{-1}\text{ soil h}^{-1}$ (Soil Pit 1, AU[hh], 42–69 cm). In the buried humus accumulation horizons (Soil Pit 2, AU[hh], 42–70 cm; Soil Pit 3, AU[hh]_{pyr}, 63–74 cm), the rates of basal respiration were at the level of these rates in the mineral horizon Q. This indicates the stabilization of organic matter

mineralization processes. In general, the rates of basal respiration correlate with the C_{org} values (the correlation coefficient was 0.8 with $p < 0.05$).

4.4. Group and Fractional Composition of Soil Organic Matter

Organic substances play a special role in the genesis and fertility of soils. Knowledge in such research makes it possible to understand the ecological and genetic aspects in the formation and transformation of organic matter and in the determination of elementary soil processes during the formation of organic soil profiles in different landscape zones. At the same time, with an increase in anthropogenic impact and climate change, the transformation of humus as an important component of soil organic matter requires additional study [51]. The content, reserves, and composition of humus are among the most important indicators that determine the ecological properties of soils. These indicators are also used in the classification, diagnosis, and assessment of soil resistance to the action of various destructive factors (erosion, deflation, fires, intensive agricultural use, and pollution with various chemicals). In turn, the impact of these factors can lead to the transformation of humic acids (HA) [28].

In the group composition in the humus horizon AU of the reference, archeological, and AU[hh] of buried soils, HA content prevails over FA content (Table 2). Among HA fractions, the HA2 fraction associated with calcium prevails. The distribution of HA/FA along the soil profile differed in all plots and was related to the peculiarities of soil formation, hydrological regime, and gleyed carbonate horizon Q. For example, in the soil of the archeological plot, HA/FA values increased with depth, with the maximum in layer AU[hh] 42–69 cm; then, they sharply decreased in horizon Q. We assumed that this was due to the migration of the water-soluble FA down profile with subsurface runoff, the infiltration of rain and snowmelt water, and accumulation in front of the impermeable gleys horizon. In contrast, the migration and decomposition of HA occurred more slowly due to the stability of this humus component. The highest value of HA/FA in 30–70 cm of the background site was probably due to the washout of FA from elevated areas and other erosion or sedimentation processes.

Table 2. Group and fractional composition of humus in the archeological site's soil.

Horizon and Sampling Depth, cm	Carbon of Humic Acids (HA) Fractions, in % to C _{org}			Carbon of Fulvic Acid (FA) Fractions, in % to C _{org}			HA/FA	Nonhydrolyzable Residue	
	1	2	3	1a	1	2			3
Soil Pit 1 (archeological site)									
AU, 0–12	13.65	20.43	10.69	1.73	9.83	0.00	0.90	3.59	42.77
AU _{rr} , 12–21	21.25	19.50	5.28	4.11	14.79	0.00	2.26	2.18	32.81
AU[hh], 21–42	5.35	30.03	9.56	1.62	6.05	3.00	1.58	3.67	42.81
AU[hh], 42–69	3.71	47.23	7.43	1.70	2.29	3.00	1.35	7.00	33.29
Q, 69–83	2.05	33.52	8.22	6.82	0.00	6.20	2.76	2.78	40.43
Soil Pit 2 (buried or sealed soil)									
AU[hh], 42–70	9.44	43.82	9.44	1.81	5.53	4.00	0.90	5.12	25.06
Q, 70–85	3.7	42.60	7.41	3.19	9.78	0.00	7.41	2.64	25.91
Soil Pit 3 (long pyrogenic exposure)									
AU[hh] _{pyr} , 63–74	9.43	21.73	6.60	8.23	5.01	9.20	3.78	1.44	36.02
Soil Pit 4 (the reference soil)									
AU, 0–30	7.93	27.52	9.72	1.41	6.8	0.00	1.68	4.57	44.94
AU, 30–70	2.05	48.93	8.80	1.45	4.37	0.00	0.88	8.92	33.52

Note. Here and in Table 3: HA1 extracted with 0.1 N NaOH, HA2—0.1 N NaOH after preliminary decalcination of the soil with 0.1 N H₂SO₄; HA3—0.02 N NaOH at six-hour heating in a water bath.

Table 3. Humus content, its type, and distribution HA fractions.

Horizon and Sampling Depth, cm	Humus, %	Type of Humus	Fractions of HA, % from Σ HA		
			1	2	3
Soil Pit 1 (archeological site)					
AU, 0–12	15.15 vh	Humate	30.5 l	45.6 m	23.9 h
AU _{rr} , 12–21	14.35 vh	Humate	46.2 m	42.4 m	11.5 m
AU[hh], 21–42	10.63 vh	Humate	11.9 vl	66.8 h	21.3 h
AU[hh], 42–69	6.50 h	Humate	6.4 vl	80.9 vh	12.7 m
Q, 69–83	2.52 l	Humate	4.7 vl	76.5 h	18.8 m
Soil Pit 2 (buried or sealed soil)					
AU[hh], 42–70	4.01 m	Humate	15.1 vl	69.9 h	15.1 m
Q, 70–85	0.93 vl	Humate	6.9 vl	79.3 h	13.8 m
Soil Pit 3 (long pyrogenic exposure)					
AU[hh] _{pyr} , 63–74	1.83 vl	Fulvate–humate	25.0 l	57.5 m	17.5 m
Soil Pit 4 (background soil)					
AU, 0–30	13.47 vh	Humate	17.6 vl	60.9 h	21.5 h
AU, 30–70	5.88 m	Humate	3.4 vl	81.9 vh	14.7 m

Note. Manifestation levels: vl—very low; l—low; m—medium; h—high; vh—very high.

The humus content in the humus horizons' AU of the archeological site and the background plot was within the average values. In the humus horizons of buried soils AU[hh], humus content ranged from low to high values (Table 3). Humus in the humus horizons of the background plot, archeological soils, and buried soils AU[hh] was of the humate type. The exception was the pyrogenic layer (AU[hh]_{pir}) from the ancient furnace, where humus is represented by the fulvate–humate type.

In the humus horizons of the buried (AU[hh]) and reference soil (AU), the HA3 fraction ranked second after the HA2 fraction in terms of the HA content, which is associated with the predominance of clay particles in this layer. In the humus horizon AU of the

archeological plot and the pyrogenic layer $AU[hh]_{pyr}$ from the ancient furnace, it was in second place (after HA2) in terms of the share of HA1 (Table 3). The proportion of HA2 had a high and very high value in the humus horizons of buried soils ($AU[hh]$) and the AU of the reference soil. In the humus horizons of the archeological site and the pyrogenic layer $AU[hh]_{pyr}$ from the ancient furnace, there was an average level of humus according to HA2. In the humus horizons of the archeological site and the pyrogenic layer $AU[hh]_{pyr}$ from the ancient furnace, the HA1 fraction and humus level corresponded to a low and very low level of manifestation (Table 3).

According to the spectrophotometric characteristics of solutions of HA in the humic horizons AU of the archeological site, the buried soils $AU[hh]$, and the pyrogenic layer $AU[hh]_{pyr}$ from the ancient furnace, the HA2 fraction was the densest, and HA1 was the least optically dense (Table 3). For the humus horizons (AU and $AU[hh]$) of the archeological site, reference, and buried soil, and in the pyrogenic layer $AU[hh]_{pyr}$ from the ancient furnace, the spectrophotometric curves of the HA2 and HA3 fractions concerning the chromaticity coefficient had a flatter arrangement, while the spectrophotometric curves of HA1 are distinguished by a greater steepness (Table 4).

Table 4. Optical density and chromaticity coefficient for HA fractions.

Horizon and Sampling Depth, cm	Optical Density, $E\ 1\ mg\ ml^{-1}$, 430 nm			Chromaticity Coefficient, $E_{465\ nm} : E_{665\ nm}$		
	1	2	3	1	2	3
Soil Pit 1 (archeological site)						
AU, 0–12	7.84	18.36	11.43	7.13	4.09	4.06
AU _{rr} , 12–21	5.51	16.98	12.82	4.18	4.33	3.67
$AU[hh]$, 21–42	17.32	26.50	20.75	5.92	3.68	3.42
$AU[hh]$, 42–69	6.33	27.10	18.61	6.57	3.58	3.51
Q, 69–83	2.08	20.58	21.48	5.69	3.98	3.67
Soil Pit 2 (buried or sealed soil)						
$AU[hh]$, 42–70	15.23	25.21	19.39	5.15	3.61	3.26
Q, 70–85	1.01	18.68	13.07	2.78	3.97	3.85
Soil Pit 3 (long pyrogenic exposure)						
$AU[hh]_{pyr}$, 63–74	12.43	19.26	16.94	5.66	4.28	3.81
Soil Pit 4 (background soil)						
AU, 0–30	13.05	25.18	15.63	6.38	3.84	3.72
AU, 30–70	4.93	27.20	20.16	7.28	3.51	3.31

Comparing the optical density curves using the example of the HA2 fraction at different wavelengths shows that HA from the humus horizon of the AU archeological plot and from the pyrogenic layer, $AU[hh]_{pyr}$ was less optically dense than the background values were (Figure 6). In terms of optical density, HA2 from the buried horizon $AU[hh]$ was close to the values of the background soil AU (Figure 6).

Analysis of the group and fractional composition of the organic matter showed that HA2 fractions, mainly associated with calcium, prevail in the reference soil. With depth, their content increases from 28% to 49%. The proportion of FA was insignificant. For example, the maximum content of the FA1 fraction did not exceed 7%. In the topsoil of the archeological site, free HA (HA1) associated with mobile sesquioxides (14–21%) and HA associated with calcium (about 20%) predominate. The proportion of FA1 also increased to 10–15%. This organic matter composition is most likely due to organic residues left after the functioning of the summer field camp of farm animals. Further, in the buried horizons (Soil Pits 1 and 2), the composition of organic matter corresponds to the reference soil. Significant changes occurred in the soil affected by fire. Most likely, it was influenced by

prolonged exposure to high temperatures and the presence of unburned organic residues (coal) and ash. The proportion of acids in the HA2 fraction decreased to 22%; all FA fractions increased: FA1a, ~8%; FA1, ~5%; FA2, ~9%; FA3, ~4%.

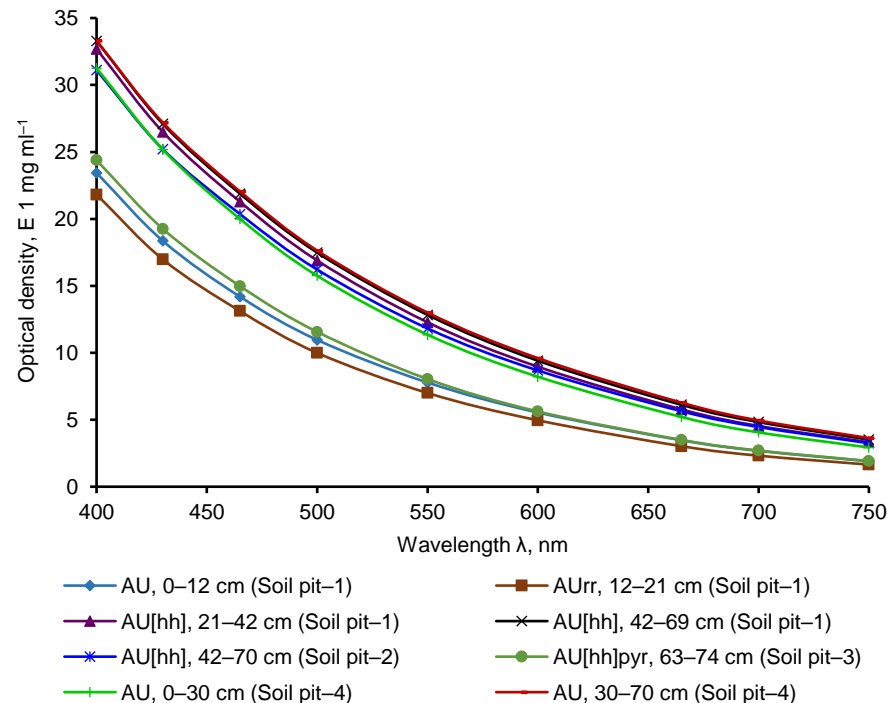


Figure 6. Curves of optical density of HA2 fraction at different wavelengths.

Significant changes also took place in the optical density of HA in the HA2 fraction. HA in humus accumulation horizons of both the reference soil (AU, Soil Pit 4) and the buried soil (AU[hh], Soil Pits 1 and 2) was the most intensely colored. HA from the AU and AUrr horizons (Soil Pit 1) of the soil at the archeological site and the pyrogenic horizon AU[hh]_{pyr} (Soil Pit 3) had less optical density. Apparently, this is also due to organic waste from the summer field camp and exposure to high temperatures.

In general, according to the spectrophotometric characteristics of solutions of HA in the humic horizons AU of all studied soils, the HA2 fraction was the densest; the HA1 fraction was the least optically dense (Table 4).

The chromaticity coefficient of couple E4:E6 (wavelength E465:E665 nm) and optical density curves could characterize the development (evolution) of molecules of organic substances [52]. When the chromaticity coefficient had low values and curves of the optical density of the HA2 fraction were gentle and concave on the axis, this means that the molecules of organic matter are “mature”. In this way, “unripe” molecules occurred in the pyrogenic layer (Soil Pit 3) and topsoil (AU and AUrr) of the archeological site. Thus, fire and human or cattle activity had a substantial effect on the age of the molecules.

5. Conclusions

Results of morphological and physicochemical studies show the anthropogenic impact on the soil at the archeological site. The newly formed AU horizon, which covered the deeper horizons at the archeological site (Soil Pit 1) and was affected by the cattle summer camp, was richer in agrochemical properties, namely, the content of exchangeable and gross forms of phosphorus, alkaline hydrolyzable nitrogen, and exchange cations of the soil absorbing complex compared to the reference soil. For the pyrogenic layer (AU[hh]_{pyr}) from the ancient furnace (Soil Pit 3), the mobile and total forms of phosphorus are several times higher than the values of the reference soil. However, they were inferior according to other agrochemical indicators.

The organic matter content in the humus horizon (AU) of the soil in the cattle summer camp is near the reference soil values. In the pyrogenic layer (AU[hh]_{pyr}) from the ancient furnace, the content was approximately seven times less than that of the background site. The humus type in the pyrogenic layer from the ancient furnace is fulvate–humate, and the humus type in the humus horizon AU (Soil Pit 1) was formed and corresponded with values in the humus horizons (AU layers) of the reference soil and the buried soils (AU[hh]). The share of the nonhydrolyzable residue in the humus horizons of buried soils (AU[hh], 25.1–42.8%) was less than the background values (AU, 33.5–44.9%). This is consistent with literature data [53] and confirms that the nonhydrolyzable residue did not accumulate after burial in the humus horizons.

Among the fractions of HA in the humus horizon (AU) of soils, the highest values were found on the territory of the cattle summer camp and in the pyrogenic layer (AU[hh]_{pyr}) from the ancient furnace. Second place was taken by the HA1 fraction, and the third by HA3. In contrast, in the humus horizons (AU) of the reference soil and in the buried humus horizons (AU[hh]), second place after HA2 was taken by HA3 (this is associated with clay particles), and the third place by the HA1 fraction.

In general, the humus horizon AU, formed within the ancient cattle summer camp, was closer to the values of the humus horizon at the reference site in terms of some agrochemical characteristics and indicators of the humus state. The pyrogenic layer (AU[hh]_{pyr}) from the ancient furnace contains the biophilic elements in increased amounts.

The current status of native (background) soils and the archeological plot' soils is in "natural mode". In particular, background soils are subject to the natural process of soil formation and not degraded while they are not in agricultural use (plowing, grazing, etc.) and not affected by negative anthropogenic impact (factories, construction, etc.); only small erosion processes probably occur on the slope. Archeological soils are buried and preserved by newly formed soil cover.

Author Contributions: Writing—original draft preparation, R.S.; conceptualization, G.O.; methodology, G.O.; software, A.S.; formal analysis, A.K., N.A., I.A. and E.A.; investigation, R.S., G.O. and N.A.; writing—review and editing, M.K. and A.G. All authors have read and agreed to the published version of the manuscript.

Funding: This study was performed within the framework of state assignment of the Ministry of Science and Education of the Russian Federation no. 075-00326-19-00 in theme no. AAA-A18-118022190102-3. This work was also supported by a grant from the Russian Science Foundation, project no. 17-16-01030, "Soil biota dynamics in chronoserries of post-technogenic landscapes: analyses of soil-ecological effectiveness of ecosystems restoration", and by the Kazan Federal University Strategic Academic Leadership Program.

Institutional Review Board Statement: Not applicable.

Informed Consent Statement: Not applicable.

Data Availability Statement: Not applicable.

Conflicts of Interest: The authors declare no conflict of interest.

References

1. Dazzi, C.; Galati, A.; Crescimanno, M.; Papa, G.L. Pedotechnique applications in large-scale farming: Economic value, soil ecosystems services and soil security. *Catena* **2019**, *181*, 104072. [[CrossRef](#)]
2. Bazarova, V.B.; Tsydenova, N.V.; Lyashevskaya, M.S.; Khenzykhenova, F.I.; Tumen, D.; Erdene, M. Reconstruction of paleoenvironmental conditions of ancient people habitation in the Togootyn Gol River valley (Eastern Mongolia). *Quat. Int.* **2019**, *503*, 105–114. [[CrossRef](#)]
3. Shtienberg, G.; Dix, J.K.; Shahack-Gross, R.; Yasur-Landau, A.; Roskin, J.; Bookman, R.; Waldmann, N.; Shalev, S.; Sivan, D. Anthropogenic overprints on natural coastal aeolian sediments: A study from the periphery of ancient Caesarea, Israel. *Anthropocene* **2017**, *19*, 22–34. [[CrossRef](#)]
4. Gong, Z.; Zhang, X.; Chen, J.; Zhang, G. Origin and development of soil science in ancient China. *Geoderma* **2003**, *115*, 3–13. [[CrossRef](#)]

5. Rothschild, N.A.; di Zerega, W.D. Urban archaeology. In *Encyclopedia of Archaeology*; Pearsall, D.M., Ed.; Academic Press: New York, NY, USA, 2008; pp. 2164–2171. Available online: <https://doi.org/10.1016/B978-012373962-9.00313-7> (accessed on 7 July 2021).
6. Li, M.; Fang, H.; Zheng, T.X.; Rosen, A.; Wright, H.; Wright, J.; Wang, Y. Archeology of the Lu City: Place memory and urban foundation in Early China. *Archaeol. Res. Asia* **2018**, *14*, 151–160. [[CrossRef](#)]
7. Macphail, R.I. Soils and archaeology. In *Encyclopedia of Archaeology*; Pearsall, D.M., Ed.; Academic Press: New York, NY, USA, 2008; pp. 2064–2072. Available online: <https://doi.org/10.1016/B978-012373962-9.00290-9> (accessed on 7 July 2021).
8. Crabtree, P.J.; Reilly, E.; Wouters, B.; Devos, Y.; Bellens, T.; Schryvers, A. Environmental evidence from early urban Antwerp: New data from archaeology, micromorphology, macrofauna and insect remains. *Quat. Int.* **2017**, *460*, 108–123. [[CrossRef](#)]
9. Wouters, B.; Devos, Y.; Milek, K.; Vrydaghs, L.; Bartholomieux, B.; Tys, D.; Moolhuizen, C.; van Asch, N. Medieval markets: A soil micromorphological and archaeobotanical study of the urban stratigraphy of Lier (Belgium). *Quat. Int.* **2017**, *460*, 48–64. [[CrossRef](#)]
10. Zubarev, V.; Smekalov, S.; Yartsev, S. Materials for the ancient landscape reconstruction in the Adzhel landscape compartment in the Eastern Crimea (the first stage research results). *J. Archaeol. Sci. Rep.* **2019**, *23*, 993–1013. [[CrossRef](#)]
11. Scudder, S.J.; Foss, J.E.; Collins, M.E. Soil science and archaeology. In *Advances in Agronomy*; Sparks, D.L., Ed.; Academic Press: New York, NY, USA, 1996; pp. 1–76. Available online: [https://doi.org/10.1016/S0065-2113\(08\)60922-0](https://doi.org/10.1016/S0065-2113(08)60922-0) (accessed on 7 July 2021).
12. Feinman, G.M. Settlement and landscape archaeology. In *International Encyclopedia of the Social and Behavioral Sciences*, 2nd ed.; Wright, J.D., Ed.; Elsevier: Amsterdam, The Netherlands, 2015; pp. 654–658. Available online: <https://doi.org/10.1016/B978-0-08-097086-8.13041-7> (accessed on 7 July 2021).
13. Nriagu, J. Environmental pollution and human health in ancient times. In *Encyclopedia of Environmental Health*, 2nd ed.; Nriagu, J., Ed.; Elsevier: Amsterdam, The Netherlands, 2019; pp. 598–614. Available online: <https://doi.org/10.1016/B978-0-12-409548-9.11756-7> (accessed on 7 July 2021).
14. Walkington, H. Soil science applications in archaeological contexts: A review of key challenges. *Earth-Sci. Rev.* **2010**, *103*, 122–134. [[CrossRef](#)]
15. Hillson, S. *Mammal Bones and Teeth. An Introductory Guide to Methods of Identification*; Institute of Archaeology, University College London: London, UK, 1999.
16. Wokken, G.G.; Glagolev, P.A.; Bogolyubsky, S.N. *Pet Anatomy. System of Organs of Movement. Part 1*; Higher school: Moscow, Russia, 1961; p. 391.
17. Klimov, A.F. *Anatomy of Domestic Animals*; Lan: Saint Petersburg, Russia, 2003; p. 1040. (In Russian)
18. Morgunova, N.L.; Vasilyeva, I.N.; Kulkova, M.A.; Roslyakova, N.V.; Salugina, N.P.; Turetskiy, M.A.; Fayzullin, A.A.; Khokhlova, O.S. *Turganik Settlement in the Orenburg Region*; OGPU: Orenburg, Russia, 2017; p. 300. (In Russian)
19. Shishlina, N.; Roslyakova, N.; Kolev, Y.; Bachura, O.; Kuznetsova, O.; Kiseleva, D.; Retivov, V.; Tereschenko, E. Animals, metal and isotopes: Mikhailo-Ovsyanka I, the Late Bronze Age mining site of the steppe Volga region. *Archaeol. Res. Asia* **2020**, *24*, 100229. [[CrossRef](#)]
20. Golyeva, A.; Khokhlova, O.; Shcherbakov, N.; Shuteleva, I. Negative effects of Bronze age human activity on modern soils and landscapes, a case-study on the Muradymovo settlement, Urals, Russia. *Interdiscip. Archaeol.* **2016**, *7*, 169–178. [[CrossRef](#)]
21. Golyeva, A.; Khokhlova, O.; Lebedeva, M.; Shcherbakov, N.; Shuteleva, I. Micromorphological and chemical features of soils as evidence of bronze age ancient anthropogenic impact (Late Bronze Age Muradymovo settlement, Ural region, Russia). *Geosciences* **2018**, *8*, 313. [[CrossRef](#)]
22. Krzewińska, M.; Kilińc, G.M.; Juras, A.; Koptekin, D.; Chyleński, M.; Nikitin, A.G.; Shcherbakov, N.; Shuteleva, I.; Leonova, T.; Kraeva, L.; et al. Ancient genomes suggest the eastern Pontic-Caspian steppe as the source of western Iron Age nomads. *Sci. Adv.* **2018**, *4*, eaat4457. [[CrossRef](#)]
23. Shuteleva, I.A.; Shcherbakov, N.B.; Balonova, M.G.; Khokhlova, O.S.; Goleva, A.A. Some results of the application of a complex approach to the research of the Late Bronze age settlement in the Volgo-Ural region. *Interdiscip. Archaeol. Nat. Sci. Archaeol.* **2010**, *1*, 29–36. [[CrossRef](#)]
24. Peel, M.C.; Finlayson, B.L.; McMahon, T.A. Updated world map of the Köppen-Geiger climate classification. *Hydrol. Earth Syst. Sci.* **2007**, *11*, 1633–1644. [[CrossRef](#)]
25. IUSS Working Group WRB. World Reference Base for Soil Resources 2014, Update 2015. International Soil Classification System for Naming Soils and Creating Legends for Soil Maps. In *World Soil Resources Reports*; FAO: Rome, Italy, 2015; p. 182.
26. Khaziev, F.K. *Soils of Bashkortostan. Vol. 1. Ecologic-Genetic and Agroproductive Characterization*; Gilem: Ufa, Russia, 1995; p. 385. (In Russian)
27. Arinushkina, E.V. *Agrochemical Methods of Soil Studies*; Nauka: Moscow, Russia, 1970; p. 656. (In Russian)
28. Orlov, D.S. *Humic Substances of Soils and General Theory of Humification*; Oxford and IBH Publishing: New Delhi, India, 1995.
29. Kononova, M.M. Soil organic matter. In *Its Nature, Its Role in Soil Formation and Soil Fertility*; Pergamon Press: Oxford, UK, 1961.
30. Vadyunina, A.F.; Korchagina, Z.A. *Methods of Studying the Physical Properties of Soils*; Agropromizdat: Moscow, Russia, 1986; p. 416. (In Russian)
31. Prikhod'ko, V.E.; Sizemskaya, M.L. Basal respiration and composition of microbial biomass in virgin and agroforest-reclaimed semidesert soils of the Northern Caspian region. *Eurasian Soil Sci.* **2015**, *48*, 852–861. [[CrossRef](#)]

32. Mohammadi, M.; Shabanpour, M.; Mohammadi, M.H.; Davatgar, N. Characterizing spatial variability of soil textural fractions and fractal parameters derived from particle size distributions. *Pedosphere* **2019**, *29*, 224–234. [[CrossRef](#)]
33. Wang, J.; Zhang, J.; Feng, Y. Characterizing the spatial variability of soil particle size distribution in an underground coal mining area: An approach combining multi-fractal theory and geostatistics. *Catena* **2019**, *176*, 94–103. [[CrossRef](#)]
34. Rubinić, V.; Lazarević, B.; Husnjak, S.; Durn, G. Climate and relief influence on particle size distribution and chemical properties of Pseudogley soils in Croatia. *Catena* **2015**, *127*, 340–348. [[CrossRef](#)]
35. Holliday, V.T.; Gartner, W.G. Methods of soil P analysis in archaeology. *J. Archaeol. Sci.* **2007**, *34*, 301–333. [[CrossRef](#)]
36. Rodrigues, S.F.S.; da Costa, M.L. Phosphorus in archeological ceramics as evidence of the use of pots for cooking food. *Appl. Clay Sci.* **2016**, *123*, 224–231. [[CrossRef](#)]
37. Fenger-Nielsen, R.; Hollesen, J.; Matthiesen, H.; Andersen, E.A.S.; Westergaard-Nielsen, A.; Harmsen, H.; Michelsen, A.; Elberling, B. Footprints from the past: The influence of past human activities on vegetation and soil across five archaeological sites in Greenland. *Sci. Total Environ.* **2019**, *654*, 895–905. [[CrossRef](#)]
38. da Costa, M.L.; Kern, D.C. Geochemical signatures of tropical soils with archaeological black earth in the Amazon, Brazil. *J. Geochem. Explor.* **1999**, *66*, 369–385. [[CrossRef](#)]
39. Migliavacca, M.; Pizzeghello, D.; Busana, M.S.; Nardi, S. Soil chemical analysis support the identification of ancient breeding structures: The case-study of Cà Tron (Venice, Italy). *Quat. Int.* **2012**, *275*, 128–136. [[CrossRef](#)]
40. Valente, G.J.S.S.; Costa, M.L. Fertility and desorption capacity of Anthrosols (Archaeological Dark Earth—ADE) in the Amazon: The role of the ceramic fragments (sherds). *Appl. Clay Sci.* **2017**, *138*, 131–138. [[CrossRef](#)]
41. Zolotareva, B.N.; Bukhonov, A.V.; Demkin, V.A. The structural state of buried and surface soils of solonchic complexes in the dry steppe zone of the Lower Volga basin. *Eurasian Soil Sci.* **2012**, *45*, 690–699. [[CrossRef](#)]
42. Zolotareva, B.N.; Demkin, V.A. Humus in paleosols of archaeological monuments in the dry steppes of the Volga-Don interfluvium. *Eurasian Soil Sci.* **2013**, *46*, 262–272. [[CrossRef](#)]
43. Wittenberg, L.; van der Wal, H.; Keesstra, S.; Tessler, N. Post-fire management treatment effects on soil properties and burned area restoration in a wildland-urban interface, Haifa Fire case study. *Sci. Total Environ.* **2020**, *716*, 135190. [[CrossRef](#)] [[PubMed](#)]
44. Gabbasova, I.M.; Garipov, T.T.; Suleimanov, R.R.; Komissarov, M.A.; Khabirov, I.K.; Sidorova, L.V.; Nazyrova, F.I.; Prostyakova, Z.G.; Kotlugalyamova, E.Y. The Influence of ground fires on the properties and erosion of forest soils in the Southern Urals (Bashkir State Nature Reserve). *Eurasian Soil Sci.* **2019**, *52*, 370–379. [[CrossRef](#)]
45. Amoako, E.E.; Gambiza, J. Effects of anthropogenic fires on soil properties and the implications of fire frequency for the Guinea savanna ecological zone, Ghana. *Sci. Afr.* **2019**, *6*, e00201. [[CrossRef](#)]
46. Francos, M.; Stefanuto, E.B.; Úbeda, X.; Pereira, P. Long-term impact of prescribed fire on soil chemical properties in a wildland-urban interface. Northeastern Iberian Peninsula. *Sci. Total Environ.* **2019**, *689*, 305–311. [[CrossRef](#)] [[PubMed](#)]
47. Gonza'lez-Pe'rez, J.A.; Gonza'lez-Vila, F.J.; Almendros, G.; Knicker, H. The effect of fire on soil organic matter—A review. *Environ. Int.* **2004**, *30*, 855–870. [[CrossRef](#)] [[PubMed](#)]
48. Gerlach, R.; Fischer, P.; Eckmeier, E.; Hilgers, A. Buried dark soil horizons and archaeological features in the Neolithic settlement region of the Lower Rhine area, NW Germany: Formation, geochemistry and chronostratigraphy. *Quat. Int.* **2012**, *265*, 191–204. [[CrossRef](#)]
49. Säurich, A.; Tiemeyer, B.; Don, A.; Fiedler, S.; Bechtold, M.; Amelung, W.; Freibauer, A. Drained organic soils under agriculture—The more degraded the soil the higher the specific basal respiration. *Geoderma* **2019**, *355*, 113911. [[CrossRef](#)]
50. Lull, C.; Bautista, I.; Lidón, A.; del Campo, A.D.; González-Sanchis, M.; García-Prats, A. Temporal effects of thinning on soil organic carbon pools, basal respiration and enzyme activities in a Mediterranean Holm oak forest. *For. Ecol. Manag.* **2020**, *464*, 118088. [[CrossRef](#)]
51. Orlov, D.S.; Grishina, L.A. *Workshop on the Chemistry of Humus*; Moscow State University: Moscow, Russia, 1981; p. 272. (In Russian)
52. Welte, E. Neuere ergebnisse der humusforschung. *Angev. Chem.* **1955**, *67*, 153–155. [[CrossRef](#)]
53. Alekseeva, T.V.; Zolotareva, B.N.; Kolyagin, Y.G. Nonhydrolyzable part of soil organic matter in buried and modern soils. *Eurasian Soil Sci.* **2019**, *52*, 632–643. [[CrossRef](#)]